Experimental Gerontology, Vol. 33, Nos. 7/8, pp. 837–851, 1998

0531-5565/98 $19.00 + .00

ELSEVIER

PII S0531-5565(98)00038-2

DIFFUSION CONSTRAINTS AND NEURON–GLIA INTERACTION DURING AGING

EVA SYKOVÁ, TOMÁŠ MAZEL and ZUZANA ŠIMONOVÁ

Department of Neuroscience, Second Medical Faculty, Charles University, V úvalu 84, Prague 150 18, and Department of Neuroscience, Institute of Experimental Medicine AS CR, Vídeňská 1083, Prague 142 20, Czech Republic

Abstract—Changes in brain extracellular space (ECS) volume, composition, and geometry are a consequence of neuronal activity, of glial K^+, pH, and amino acid homeostasis, and of changes in glial cell morphology, proliferation, and function. They occur as a result of repetitive neuronal activity, seizures, anoxia, injury, inflammation, and many other pathological states in the CNS, and may significantly affect signal transmission in the CNS. Activity-related or CNS damage-related cellular swelling is compensated for by ECS volume shrinkage and, as a consequence, by a decrease in the apparent diffusion coefficients (ADCs) of neuroactive substances diffusing in the ECS. Changes in cellular morphology, such as occur during aging, could also result in changes of ECS volume and geometry. We provide evidence for limited diffusion in rat cortex, corpus callosum, and hippocampus in the aging brain that correlates with changes in glial volume and the extracellular matrix. In all structures, the mean ECS volume fraction α (α = ECS volume/total tissue volume) and nonspecific uptake k' are significantly lower in aged rats (26–32 months old) than in young adult brain. Compared to young adult brain, in the aged brain we found an increase in GFAP staining and hypertrophied astrocytes with thicker processes which, in the hippocampus, lost their radial organization. The tortuosity ($\lambda = \sqrt{D/ADC}$) was lower in the cortex and CA3 region. Immunohistochemical staining for fibronectin and chondroitin sulfate proteoglycans revealed a substantial decrease that could account for a decrease in diffusion barriers. Diffusion parameters α, λ, and k' in the aging brain after cardiac arrest changed substantially faster than in the young adult brain, although the final values were not significantly different. This suggests that the smaller extracellular space during aging results in a greater susceptibility of the aging brain to anoxia/ischemia, apparently due to a faster extracellular acidosis and accumulation of K^+ and toxic substances, for example, glutamate. We conclude that during aging the movement of substances is more hindered in the narrower clefts. This is partly compensated for by a decrease in the diffusion barriers that may be formed by macromolecules of the extracellular matrix. Diffusion parameters can affect the efficacy of synaptic as well as extrasynaptic transmission by a greater accumulation of substances, because they diffuse away from a source more slowly, or induce damage to nerve cells if these substances reach toxic concentrations.

Correspondence to: Eva Syková, Institute of Experimental Medicine AS CR, Department of Neuroscience, Videňská 1083, Prague, 142 20, Czech Republic; Fax: +420-2-475-27-83; E-mail: sykova@biomed.cas.cz

Diffusion parameters are also of importance in the "crosstalk" between synapses, which has been hypothesized to be of importance during LTP and LTD. We can, therefore, assume that the observed changes in ECS diffusion parameters during aging can contribute to functional deficits and memory loss.

Key Words: apparent diffusion coefficient, astrogliosis, extracellular space, extrasynaptic transmission, hippocampus, tortuosity, volume fraction, volume transmission

INTRODUCTION

COGNITIVE FUNCTIONS, particularly memory formation, show substantial decline in old age. Age-related differences in brain activity may reflect atrophy, neuronal death, depletion of transmitter release, and synaptic activity, and other, sometimes only subtle, structural changes. These include astrogliosis and changes in the extracellular matrix and the macromolecular content, for example, proteoglycans. Recent quantification of neuronal loss in the hippocampus of aged rats with spatial learning deficits revealed a preserved neuron number, demonstrating that hippocampal neuronal degeneration is not an inevitable consequence of normal aging, and that a loss of principal neurons in the hippocampus fails to account for age-related learning and memory impairment (Rapp and Gallagher, 1996; Wickelgren, 1996).

Astrocytic gliosis represents a consistent finding in the cortex and hippocampus of the rodent nervous system during aging (Geinisman *et al*., 1978; Lindsey *et al*. 1979; Adams and Jones, 1985). Increased GFAP staining and an increase in the size and fibrous character of astrocytes have been repeatedly demonstrated (Goss *et al*., 1991; O'Callaghan and Miller, 1991; Nichols *et al*., 1993). It is well known that astrogliosis and astroglial swelling may affect the regulation of ionic homeostasis in the extracellular space (Syková, 1992, 1997; Norenberg, 1994). Reactive astrocytes produce a variety of cell adhesion and extracellular matrix molecules. All of these changes, which also take place in the aging brain, would substantially affect the diffusion of neuroactive substances in aged brain.

Cells, nerve fibers, and blood vessels fill about 80% of the nervous tissue volume, and the remaining 20% is the extracellular space (ECS). The ECS contains ions, neuroactive substances, i.e., transmitters, metabolites, peptides, and neurohormones, and molecules of the extracellular matrix. The ECS is not only the microenvironment of the nerve cells but also an important communication channel (Nicholson, 1980; Syková, 1983, 1992; Agnati *et al*., 1995). Populations of neurons can interact either by synapses or by the diffusion of ions and neurotransmitters in the ECS. Because glial cells do not have synapses, their communication with neurons is solely mediated by the diffusion of ions and neuroactive substances in the ECS. This extrasynaptic transmission has also been called "diffusion transmission" (neuroactive substances diffuse through the ECS) or "volume transmission" (neuroactive substances move through the volume of the ECS) (Fuxe and Agnati, 1991). Such communication without synapses may provide a mechanism for information processing in mass functions such as chronic pain, sleep, hunger, vigilance, depression, or plastic changes and memory formation. The size and irregular geometry of diffusion channels in the ECS (the so-called tortuosity, see below) substantially affect the diffusion of all neuroactive substances in the CNS, and thereby modulate neuronal signaling and neuron–glia communication. Changes in ECS diffusion parameters could result in impaired signal transmission, neuronal damage, and also contribute to functional deficits during aging.

Because extrasynaptic transmission, mediated by the diffusion of neuroactive substances (including ions, neurotransmitters, neuromodulators, growth factors, and other macromolecules) through the extracellular space, plays an important role in short- and long-distance communi-

cation between neurons, axons and glia (Agnati *et al*., 1995; Syková, 1997; Nicholson and Syková, 1998), we studied ECS diffusion parameters during aging. The real-time iontophoretic tetramethylammonium (TMA^+) method (Nicholson and Phillips, 1981) was used to determine the extracellular space volume fraction α (α = ECS volume/total tissue volume), tortuosity λ ($\lambda = \sqrt{D/ADC}$), where D is the free diffusion coefficient and ADC is the apparent diffusion coefficient of TMA^+ in the brain), and nonspecific uptake k'. The tortuosity factor describes how the migration of molecules is slowed down by pore geometry, macromolecules, or fixed negative surface charges. TMA^+ is a small cation (74.1 MW) that is restricted to the extracellular compartment and mimics the extracellular diffusion of small neuroactive molecules, ions, and metabolites. The real-time iontophoretic method is based on fitting the time-dependent rise and fall of the extracellular concentration of TMA^+ to a radial diffusion equation modified to account for extracellular volume fraction and tortuosity (Nicholson and Phillips, 1981). Recently, hypotheses concerning glutamate "spillover" and crosstalk between synapses, in which diffusion might play an important role, and their importance for LTP and LTD have been formulated, and experimental evidence for their existence was found in the hippocampus (Kullmann *et al*., 1996; Asztely *et al*., 1997; Kullmann and Asztely, 1998). Diffusion measurements performed in the cortex, corpus callosum, and hippocampus of young adult and aged rats were, therefore, compared with astrocyte morphology and changes in the extracellular matrix. Moreover, we compared the time course of the changes in ECS diffusion parameters in young adult and aged rats during ischemia.

MATERIALS AND METHODS

Experiments were performed on young adult (three- to four-month-old) and aged (26–32-month-old) male and female Wistar rats. Rats were anesthetized with an IP injection of sodium pentobarbital (65 mg/kg), and additional small doses were used to maintain the anesthesia during the experiment. The skull was opened with a dental drill 3–4 mm caudal from the bregma, 2–3 mm lateral from the midline, and the dura removed. The animal was secured in a stereotaxic apparatus on a heated platform to maintain body temperature at 37–38°C. Artificial cerebrospinal fluid with 1 mM TMA chloride heated to 37°C was continually dripped onto the surface of the exposed skull to make a small pool over the brain surface. The animals breathed spontaneously.

Double-barreled ion-selective electrodes were fabricated as described previously (Syková *et al*., 1994; Voříšek and Syková, 1997b). The tip of the ion-sensing barrel was filled with K^+ exchanger (Corning 477317), and the rest of the channel was back-filled with 100 mM TMA chloride. The reference barrel contained 150 mM NaCl. After pulling, the shank of the iontophoretic micropipette was bent so that it could be aligned parallel to that of the ion-selective microelectrode and was back-filled with 100 mM TMA chloride. An electrode array was made by gluing together a TMA^+-selective microelectrode and an iontophoresis pipette with a tip separation of 100–200 μm, allowing us to measure either in the *x*-, *y*-, or *z*-axes (Fig. 1). Gluing together two iontophoresis pipettes with a TMA^+-selective micropipette in such a way that the tips of the micropipettes and the TMA^+-selective microelectrode formed a right angle, allowed us to measure simultaneously in either *x* and *y* (Fig. 2) or *x* and *z* or *y* and *z* directions. Typical iontophoresis parameters were +20 nA bias current (continuously applied to maintain a constant transport number), with +80 nA current steps of 60-s duration to generate the diffusion curve (Figs. 1 or 2). Potentials recorded with the reference barrel were subtracted

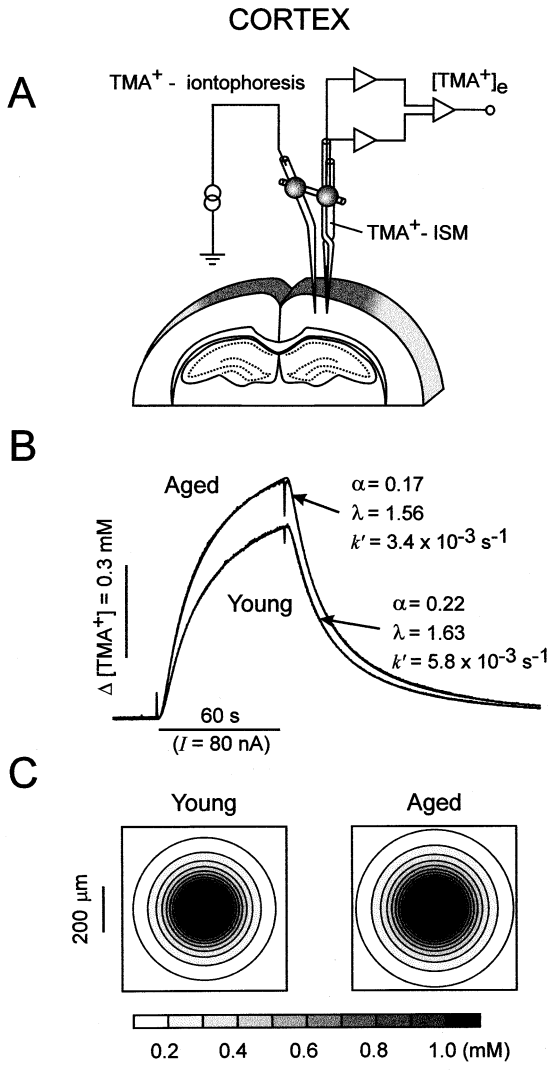

FIG. 1. Experimental setup and typical diffusion curves in the cortical layer V (A) Schema of the experimental arrangement. A TMA^+-selective double-barreled microelectrode was glued to an iontophoresis microelectrode to allow for measurements of TMA^+ diffusion curves (concentration–time profiles). (B) TMA^+ diffusion curves were measured with the same microelectrode array in the young adult rat and in the aged rat. The slower rise in the young rat means higher tortuosity and more restricted diffusion. The amplitude of the curves shows that TMA^+ concentration, at the same distance from the tip of the iontophoresis electrode, is much higher in the aged rat than in young rat. Note that the ECS volume fraction α is higher in the young rat than in an aged one. (C) Two-dimensional isoconcentration plots of extracellular TMA^+ concentration 60 s after iontophoretic application of TMA^+; measurements were done simultaneously in the *x*- and *y*-axes. The isoconcentration plots were calculated using the actual diffusion parameters (α, λ, and k'). Gray densities represent different concentrations of TMA^+ from 0.1 to 1.0 mM reached 60 s after the onset of iontophoretic application (80 nA) of TMA^+ in the middle of the circle ($D = 1.311 \times 10^{-9}\ m^2\ s^{-1}$ at 37°C, $n = 0.3$). Circles show the diffusion isotropy in the cortex of the young adult as well as the aged rat.

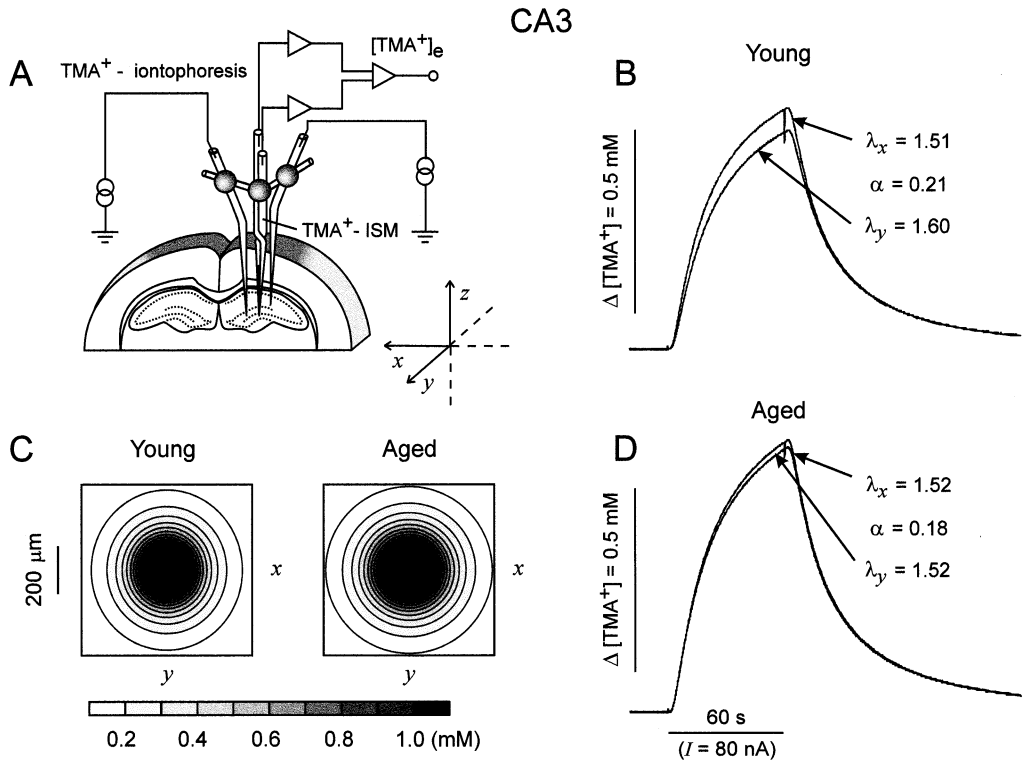

FIG. 2. Experimental setup and typical diffusion curves in the hippocampus. (A) Schema of the experimental arrangement. A TMA^+-selective double-barreled microelectrode was glued to two iontophoresis microelectrodes to allow for simultaneous measurements in the *x*- and *y*-axes. (B) Anisotropic diffusion in CA3 of a young adult rat. TMA^+ diffusion curves (concentration–time profiles) were measured along two orthogonal axes (*x*—transversal, and *y*—sagittal). The slower rise in the *y* than in the *x* direction means higher tortuosity and more restricted diffusion. The amplitude of the curves shows that TMA^+ concentration, at approximately the same distance from the tip of the iontophoresis electrode, is much higher along the *x*-axis than along the *y*-axis. This can be explained if we realize that TMA^+ concentration decreases with the "diffusion distance" from the iontophoretic micropipette, and that the real "diffusion distance" is not *r* but λr. Note that the actual ECS volume fraction α is about 0.2 and can be calculated only when measurements are done in the *x*-, *y*-, and *z*-axes using eq. 2. (C) Two-dimensional isoconcentration plots of extracellular TMA^+ concentration 60 s after iontophoretic application of TMA^+; measurements were done simultaneously in the *x*- and *y*-axes. The isoconcentration plots were calculated using the actual diffusion parameters (α, λ, and k') shown in B and D. Gray densities represent different concentrations of TMA^+ from 0.1 to 1.0 mM reached 60 s after the onset of iontophoretic application (80 nA) of TMA^+ in the middle of the circle (aged rat) or ellipse (young adult rat) ($D = 1.311 \times 10^{-9}\ m^2\ s^{-1}$ at 37°C, $n = 0.3$). Ellipses show that diffusion was anisotropic in the hippocampal CA3 of young adult rat. (D) Isotropic diffusion in CA3 of an aged rat. Note the same rise time in the *x*- and *y*-axes. Diffusion curves are higher than in B, showing that α is smaller.

from the TMA^+-selective barrel voltage measurements by means of buffer and subtraction amplifiers.

TMA^+ concentration-vs.-time curves were first recorded in 0.3% dilute agar gel (Difco, Agar Noble) in 150 mM NaCl, 3 mM KCl, and 1 mM TMA chloride to determine the transport

number (n) and the free TMA^+ diffusion coefficient (D). For the in vivo measurements the reference baseline (voltage corresponding to 1 mM TMA^+) was first read in solution above the brain, and then the array was lowered into the brain (Mazel *et al*., 1998). The diffusion curves obtained from the cortex, corpus callosum (CC), and hippocampus were analyzed to yield the volume fraction α, tortuosity λ_x, λ_y, λ_z in three perpendicular directions and the nonspecific uptake term, k' (s^{-1}). These three parameters were extracted by a nonlinear curve-fitting simplex algorithm operating on the diffusion curve described by eq. (1), which represents the behavior of TMA^+ when the iontophoresis current is applied for duration S. In this expression, C_i is the extracellular concentration of the ion at time t and distance r_i from the source in the i direction (j and k being perpendicular to i). The equation governing diffusion in brain tissue is (Nicholson and Phillips, 1981):

$$C_i = G_i(t) t < S \text{ for the rising phase of the curve}$$

$$C_i = G_i(t) - G_i(t - S) t > S \text{ for the falling phase of the curve}$$

The function G_i (u) is evaluated by substituting t or $t - S$ for u in the following equation:

$$G_i(u) = (Q\lambda_j\lambda_k/8\pi D\alpha r_i) \{\exp[r_i\lambda_i(k'/D)^{1/2}] \operatorname{erfc}[r_i\lambda_i/2(Du)^{1/2} + (k'u)^{1/2}] + + \exp[-r_i\lambda_i(k'/D)^{1/2}] \operatorname{erfc}[r_i\lambda_i/2(Du)^{1/2} - (k'u)^{1/2}]\}. \quad (1)$$

The quantity of TMA^+ delivered to the tissue per second is $Q = In/zF$, where I is the step increase in current applied to the iontophoresis electrode, n is the transport number, z is the number of charges associated with substance iontophoresed (+1 here), and F is Faraday's electrochemical equivalent. The function "erfc" is the complementary error function. When the experimental medium is agar, by definition, $\alpha = 1 = \lambda$, and $k' = 0$, and the parameters n and D are extracted by the curve fitting. Knowing n and D, the parameters α, λ, and k' can be obtained when the experiment is repeated in the brain.

The volume fraction α has to be calculated using all three curves. In our measurements we obtained the following values: α_x, α_y, α_z, λ_x, λ_y, and λ_z. α was then calculated using the following expressions (Rice *et al*., 1993; Mazel *et al*., 1998):

$$\alpha = \alpha_x(\lambda_y\lambda_z/\lambda_x^2) = \alpha_y(\lambda_x\lambda_z/\lambda_y^2) = \alpha_z(\lambda_x\lambda_y/\lambda_z^2). \quad (2)$$

After the experiment the animals were perfused, their brains were examined histologically, and the position of the microelectrode track was determined.

Immunohistochemistry

Immunohistochemical and morphological studies were undertaken on 12 young adult and 8 aged rats. Their brains were fixed with 4% paraformaldehyde, frozen sections (40 μm) were cut, and selected sections were immunostained or stained with cresyl violet (Nissl). Astrocytes were identified using monoclonal antibodies to GFAP (Boehringer-Mannheim, Germany). Immunostaining for chondroitin sulfate proteoglycans was done using CS-56 antibody (Sigma); for fibronectin we used antifibronectin antibody to a cell-attachment fibronectin fragment (Boehringer-Mannheim, Germany). After overnight incubation in the primary antibodies at 4°C, the floating sections were washed and processed using biotinylated antimouse secondary antibodies and the peroxidase-labeled avidin–biotin complex method (Vectastain Elite, Vector Laboratories, Burlingame, CA). Immune complexes were visualized using 0.05% 3,3′-diaminobenzidine tetrachloride (Sigma).

RESULTS

Diffusion parameters

The ECS diffusion parameters α, $\lambda_{x,y,z,}$ and k' were measured in cortex, corpus callosum, and in three hippocampal regions—CA1, gyrus dentatus inner blade (GD), and CA3 of young adult rats and aged rats. If diffusion in a particular brain region is anisotropic, then the correct value of the extracellular space volume fraction cannot be calculated from measurements done only in one direction. For anisotropic diffusion, the diagonal components of the tortuosity tensor are not equal, and generally its nondiagonal components need not be zero. Nevertheless, if a suitable referential frame is chosen (i.e., if we measure in three privileged orthogonal directions), neglecting the nondiagonal components becomes possible, and the correct value of the ECS size can thus be determined (Rice *et al*., 1993). Anisotropy has been already demonstrated in young adult rats in hippocampus (Mazel *et al*., 1998), corpus callosum (Voříšek and and Syková, 1997a), in myelinated spinal cord white matter (Prokopová *et al*., 1997) and in cerebellum (Rice *et al*., 1993). Anisotropic diffusion would allow for some degree of specificity in extrasynaptic transmission. Therefore, we measured TMA^+ diffusion in the ECS independently in three orthogonal axes (*x*—transversal, *y*—sagittal, *z*—vertical). Table 1 shows that the ECS volume fraction (α) in young adult rats is about the same in all brain regions studied, ranging from 0.21 to 0.22. In all these regions—cortex, corpus callosum, and hippocampus—α is significantly lower in aged animals, ranging from 0.17 to 0.19. Figure 1B shows that the diffusion curve obtained in aged cortex is higher than that in young adult rat.

Previous studies have already revealed that diffusion in young adult rat cortex is isotropic, while in corpus callosum and hippocampus it is anisotropic (Voříšek and Syková, 1997a; Mazel *et al*., 1998). Table 1 shows that in cortex, λ_x, λ_y, and λ_z have about the same values, ranging from 1.59 to 1.61. In corpus callosum λ_x is significantly lower than λ_y and λ_z, showing that the preferential TMA^+ diffusion is along the *x*-axis ($\lambda_x = 1.47$, see Table 1). Diffusion is slowed down along the *y* (sagittal)- and *z* (vertical)-axes ($\lambda_y = 1.67$, $\lambda_z = 1.69$). Diffusion anisotropy in the hippocampus in CA1, CA3, and GD reveals three different values of λ (Table 1). TMA^+ diffusion is preferential along the *x*-axis, significantly slower along the *y*-axis (Fig. 2B), and even significantly slower still along the *z*-axis than along the *y*-axis. If the diffusion is anisotropic, the real volume fraction α has to be calculated using all three diffusion curves (see expression 2). The curve obtained in the *x* direction is higher than that in the *y*, and also has the fastest rise and fall; this means that the diffusion path in this *x* direction is shorter (i.e., the tortuosity is lower) than that in *y*, though the actual distance between the electrode tips is the same in both cases (Fig. 2B). In anisotropic tissue the values of α_x, α_y, and α_z are substantially different from the actual ECS volume fraction α. It is, therefore, evident that neglecting anisotropy and measuring α in only one direction must lead to incorrect values.

Figure 2B and D shows the diffusion curves recorded in the CA3 region of hippocampus in two perpendicular axes in the young adult rat and the aged rat. It is evident that the diffusion curves for the hippocampus are larger in the aged rat than in the young one (the same electrode array was used in both cases). Although the mean tortuosity values were not significantly different between young and aged rats (except for a significantly lower λ_y in the CA3 region), they had a tendency to be lower in aged rats in the *y*- and *z*-axes (Table 1). In some aged rats the anisotropy was completely lost (Fig. 2D), i.e, the values of λ_x and λ_y, or λ_z were the same. This means that there could be a loss of anisotropy in aging hippocampus. Table 1 also shows that the average tortuosity $\lambda_{x,y,z}$ in the hippocampus (averaging λ_x, λ_y, and λ_z) is significantly lower in aging rats compared to young ones.

TABLE 1. ECS DIFFUSION PARAMETERS IN YOUNG ADULT AND AGED RAT CORTEX, CORPUS CALLOSUM, AND HIPPOCAMPUS

Structure	*Young adult rats*	*Aged rats*
Cortex (laminae IV, V, VI)	$\alpha = 0.215 \pm 0.003$	$\alpha = 0.185 \pm 0.004^{\dagger}$
	$\lambda_x = 1.591 \pm 0.007$	$\lambda_x = 1.557 \pm 0.010^{\dagger}$
	$\lambda_y = 1.610 \pm 0.008$	$\lambda_y = 1.593 \pm 0.019$
	$\lambda_z = 1.598 \pm 0.011$	$\lambda_z = 1.570 \pm 0.023$
	$\lambda_{x,y,z} = 1.602 \pm 0.004$	$\lambda_{x,y,z} = 1.569 \pm 0.006^{\dagger}$
	$k' = 4.9 \pm 0.2\ (\times 10^{-3}\ s^{-1})$	$k' = 3.5 \pm 0.2\ (\times 10^{-3}\ s^{-1})^{\dagger}$
	$n = 59$	$n = 24$
Corpus callosum	$\alpha = 0.209 \pm 0.006$	$\alpha = 0.187 \pm 0.007^{*}$
	$\lambda_x = 1.470 \pm 0.014$	$\lambda_x = 1.475 \pm 0.015$
	$\lambda_y = 1.674 \pm 0.018^{\S}$	$\lambda_y = 1.686 \pm 0.052^{\S}$
	$\lambda_z = 1.692 \pm 0.015^{\S}$	$\lambda_z = 1.710 \pm 0.044^{\S}$
	$\lambda_{x,y,z} = 1.613 \pm 0.007$	$\lambda_{x,y,z} = 1.624 \pm 0.013$
	$k' = 3.5 \pm 0.2\ (\times 10^{-3}\ s^{-1})$	$k' = 3.5 \pm 0.2\ (\times 10^{-3}\ s^{-1})$
	$n = 32$	$n = 14$
CA1	$\alpha = 0.214 \pm 0.004$	$\alpha = 0.186 \pm 0.004$
	$\lambda_x = 1.479 \pm 0.012$	$\lambda_x = 1.491 \pm 0.018$
	$\lambda_y = 1.606 \pm 0.016^{\S}$	$\lambda_y = 1.591 \pm 0.031^{\S}$
	$\lambda_z = 1.782 \pm 0.022^{\S}$	$\lambda_z = 1.715 \pm 0.022^{\S}$
	$\lambda_{x,y,z} = 1.622 \pm 0.006$	$\lambda_{x,y,z} = 1.599 \pm 0.010$
	$k' = 4.1 \pm 0.1\ (\times 10^{-1}\ s^{-1})$	$k' = 3.5 \pm 0.2\ (\times 10^{-3}\ s^{-1})$
	$n = 66$	$n = 24$
Dentate gyrus—inner blade	$\alpha = 0.225 \pm 0.008$	$\alpha = 0.190 \pm 0.008^{*}$
	$\lambda_x = 1.495 \pm 0.024$	$\lambda_x = 1.512 \pm 0.033$
	$\lambda_y = 1.593 \pm 0.029^{\ddagger}$	$\lambda_y = 1.543 \pm 0.058$
	$\lambda_z = 1.684 \pm 0.051^{\S}$	$\lambda_z = 1.686 \pm 0.074$
	$\lambda_{x,y,z} = 1.591 \pm 0.013$	$\lambda_{x,y,z} = 1.581 \pm 0.024$
	$k' = 4.9 \pm 0.4\ (\times 10^{-3}\ s^{-1})$	$k' = 3.7 \pm 0.3\ (\times 10^{-3}\ s^{-1})$
	$n = 17$	$n = 9$
CA3	$\alpha = 0.210 \pm 0.005$	$\alpha = 0.177 \pm 0.008^{\dagger}$
	$\lambda_x = 1.514 \pm 0.022$	$\lambda_x = 1.515 \pm 0.017$
	$\lambda_y = 1.601 \pm 0.018^{\S}$	$\lambda_y = 1.517 \pm 0.045^{*}$
	$\lambda_z = 1.695 \pm 0.028^{\S}$	$\lambda_z = 1.662 \pm 0.070$
	$\lambda_{x,y,z} = 1.603 \pm 0.009$	$\lambda_{x,y,z} = 1.566 \pm 0.016^{*}$
	$k' = 5.0 \pm 0.3\ (\times 10^{-3}\ s^{-1})$	$k' = 3.8 \pm 0.2\ (\times 10^{-3}\ s^{-1})$
	$n = 31$	$n = 11$

α, ECS volume fraction; λ_x, λ_y, λ_z, ECS tortuosity in the *x*-, *y*-, and *z*-direction; $\lambda_{x,y,z}$ mean ECS tortuosity; k', nonspecific TMA^+ uptake; *n*, number of measurements. Data are expressed as mean ± SEM.
$^{*}p < 0.05$; $^{\dagger}p < 0.01$; significant difference between young adults and aged rats.
$^{\ddagger}p < 0.05$; $^{\S}p < 0.01$; significant difference between tortuosity along *y*- and *x*-, or *z*- and *x*-axis.

The three-dimensional pattern of diffusion away from a point source can be illustrated by constructing iso-concentration circles (isotropic diffusion) or ellipses (anisotropic diffusion) for extracellular TMA^+ concentration. The circles and ellipses shown in Figs. 1 and 2 represent the locations where TMA^+ concentration reached 0.1, 0.2, 0.3, 0.4, 0.5, 0.6, 0.7, 0.8, 0.9, and 1 mM (represented in the gray scale) 60 s after the initiation of an 80-nA iontophoresis current. We used the actual values obtained in experiments in which the electrodes were aligned in the *x* and *y* directions. The smaller ECS volume fraction in aged rats is reflected in the larger circle or ellipse. Circles in the cortex of both young and aged rats reflect the ability of particles to diffuse

equally along the *x*-, *y*-, and *z*-axes (Fig. 1C). The ellipse in the hippocampus of the young adult rat reflects the different abilities of substances to diffuse along the *x*- and *y*-axes, while the circle in the hippocampus CA3 region of the aged rat shows isotropic diffusion (Fig. 2C).

Morphological changes

Morphological changes during aging include cell loss, loss of dendritic processes, demyelination, astrogliosis, swollen astrocytic processes, and changes in the extracellular matrix. It is reasonable to assume that there is a significant decrease in the ADC of many neuroactive substances in the aging brain, which accompanies astrogliosis and changes in the extracellular matrix. One of the explanations why α in the cortex, corpus callosum, and hippocampus of senescent rats is significantly lower than in young adults could be astrogliosis in the aged brain. Increased GFAP staining and an increase in the size and fibrous character of astrocytes have been repeatedly demonstrated (Goss *et al*., 1991, O'Callaghan and Miller, 1991; Nichols *et al*., 1993). Indeed, we found thicker GFAP-positive processes and enlarged astrocytic bodies in the cortex, CC, and hippocampus of senescent rats, which may account for changes in the ECS volume fraction (not shown). Other changes could account for the decreases in λ values, and for the disruption of tissue anisotropy. In the hippocampus in CA1, CA3, as well as in DG, we observed changes in the arrangement of fine astrocytic processes. These are normally organized in parallel in the *x*-*y* plane (Fig. 3A), and this organization totally disappears during aging (Fig. 3B). Moreover, the decreased staining for chondroitin sulfate proteoglycans and for fibronectin (Fig. 3C and D) suggests a loss of extracellular matrix macromolecules.

Ischemia

Pathological states, for example, anoxia/ischemia, are accompanied by a lack of energy, the excessive release of transmitters and neuroactive substances, glial swelling, the production of damaging metabolites including free radicals, and the loss of ionic homeostasis. It is, therefore, evident that they will be accompanied not only by substantial changes in ECS ionic composition but also by various changes in ECS diffusion parameters (Syková *et al*., 1994; Voříšek and Syková, 1997b).

Dramatic K^+ and pH_e changes occur in the brain and spinal cord during anoxia and/or ischemia. Within one minute after cardiac arrest in young adult rats, blood pressure begins to increase and pH_e begins to decrease (by about 0.1 pH unit), while $[K^+]_e$ is still unchanged. With the subsequent blood pressure decrease, the pH_e decreases by 0.6–0.8 pH unit to pH 6.4–6.6 (Fig. 4). This pH_e decrease is accompanied by a steep rise in $[K^+]_e$ to about 70 mM; decreases in $[Na^+]_e$ to 48–59 mM, $[Cl^-]_e$ to 70–75 mM; $[Ca^{++}]_e$ to 0.06–0.08 mM; an accumulation of excitatory amino acids; negative DC slow potential shift (Fig. 4); a decrease in the ECS volume fraction to 0.04–0.07; and an increase in tortuosity to 2.0–2.2. The ECS volume fraction starts to decrease when blood pressure drops below 80 mmHg and $[K^+]_e$ rises above 6 mM (Syková *et al*., 1994).

Because α is lower in aging rats, we expected some differences in the ECS diffusion parameter changes during ischemia in senescent rats. Our study revealed that the final values of α, λ, and k' induced by cardiac arrest are not significantly different; however, the time course of all the changes is faster (Fig. 5). Figure 5 shows that the first peak in TMA^+ baseline changes, indicating ECS volume decrease and K^+ increase, is reached in young adult rats at 2.9 ± 0.3 min (mean $\pm$ SEM, $n = 5$), while in senescent rats the time to peak was significantly shorter 1.5 ± 0.2 min ($n = 9$, $p = 0.0059$). The second and final peak in the TMA^+ baseline, associated

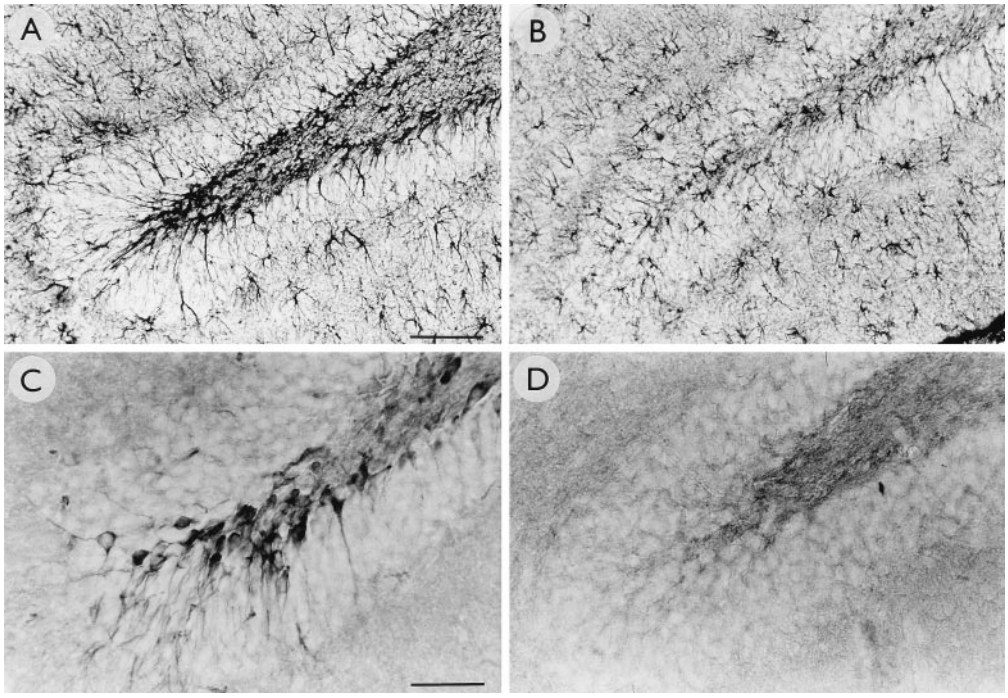

FIG. 3. Structural changes in the hippocampus gyrus dentatus region of aged rats. (A) Astrocytes stained for GFAP in the young adult rat; note the radial organization of astrocytic processes between the pyramidal cells (not stained). (B) In the aged rat the radial organization of astrocytic processes is lost. (C) Staining for fibronectin in the young adult rat shows densely stained cells, apparently due to perineuronal staining around granular cells. (D). In the aged rat the fibronectin staining is lost. Scale bar: in A and B = 100 μm; C and D = 50 μm.

with an extracellular acid shift, is reached in young adult rats at 20.2 ± 2.6 min ($n = 8$), while in senescent rats this time to peak was again significantly shorter 11.7 ± 1.8 min ($n = 9$, $p = 0.0165$). The faster changes in extracellular space volume fraction and tortuosity in nervous tissue during aging can contribute to a faster impairment of signal transmission, for example, due to a faster accumulation of ions and neuroactive substances released from cells and their slower diffusion away from the hypoxic/ischemic area in the more compacted ECS.

DISCUSSION

Our study employing the TMA^+ method shows significant differences in extracellular diffusion in the young adult and aging rat cortex, corpus callosum, and hippocampus. In young adult rats we confirm previous findings in rat brain in vivo (Mazel *et al*., 1998) that α is about 0.20 in all regions, and that diffusion is isotropic in the cortex and anisotropic in the corpus callosum, with preferential diffusion along the myelinated fibers (Vořišek and Syková, 1997b). The studies that reported a very low volume fraction α, mainly in the hippocampus (McBain *et al*., 1990), did not consider the possible anisotropy of the hippocampus, and the measurements were not done in all three axes. Moreover, measurements done in vitro could be burdened with possible artifacts, resulting from the propensity of some areas of the hippocampus to anoxia.

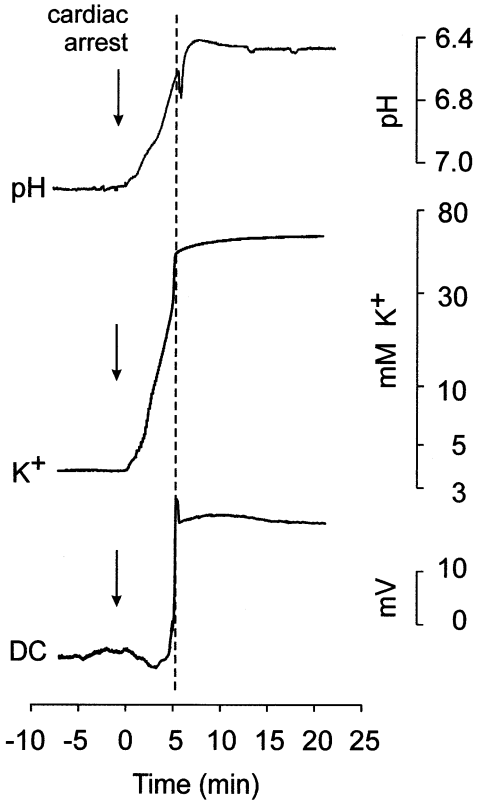

FIG. 4. Changes of extracellular pH, K^+ and anoxic depolarization (DC shift) in the cortex of the young adult rat after cardiac arrest. Recordings of extracellular pH using double-barreled pH-sensitive microelectrodes and of extracellular K^+ concentration and DC shift (anoxic depolarization) recorded simultaneously with another double-barreled K^+-selective microelectrode. Note that the first peaks in pH, K^+ concentration change, and DC shift are reached in the same time (dashed line). (After Voříšek and Syková, 1997b).

One of the most important results of the present study is the significant decrease in ECS volume fraction in all the studied structures (cortex, corpus callosum, and hippocampus) during aging. Volume fraction is also different in early postnatal development (Lehmenkühler *et al*., 1993; Voříšek and Syková, 1997b) when, in contrast to aging, ECS volume is substantially higher than in adult rat (Syková *et al*., 1996).

Astrogliosis during aging could account for the decrease in ECS volume observed in this study and in others (Syková *et al*., 1996), particularly because astrocytes outnumber neurons in many brain regions. On the other hand, the decrease in tortuosity and disappearance of anisotropy in the aging brain might also be explained by the loss of fine astrocytic processes that mingle intimately with those of neurons (Fig. 3A and B) and by a loss of extracellular matrix and perineuronal nets. Indeed, we observed a loss of fibronectin (Fig. 3C and D) and chondroitin sulfate proteoglycan staining in the hippocampus.

Chondroitin sulfate proteoglycans participate in multiple cellular processes (Hardington and Fosang, 1992; Margolis and Margolis, 1993). These include the structural regulation of the

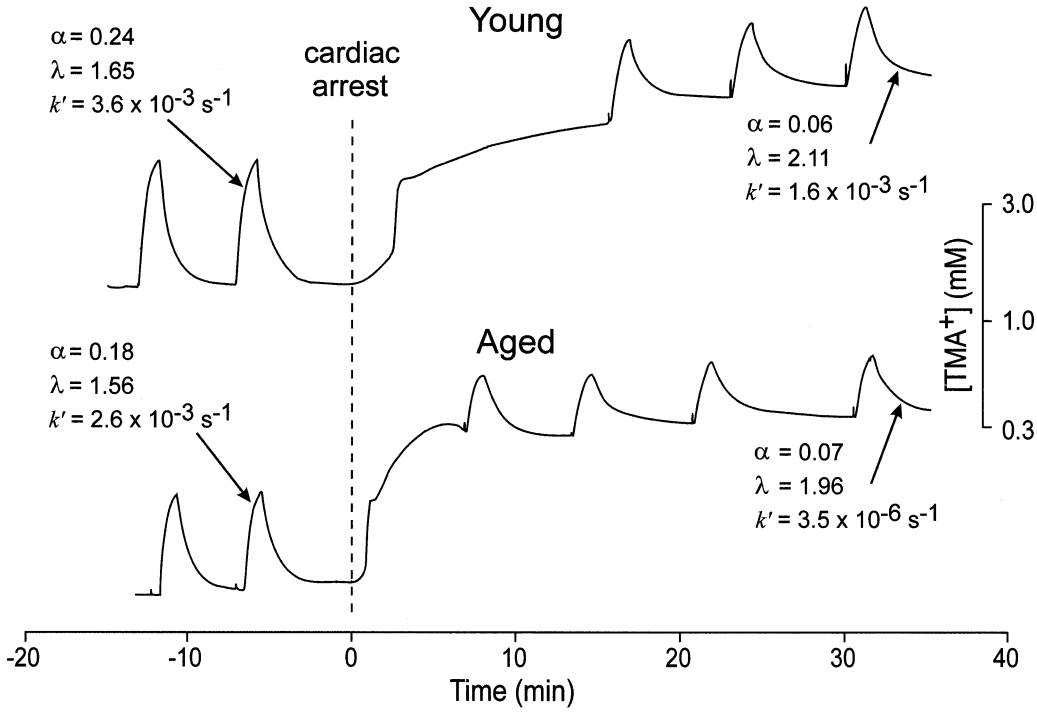

FIG. 5. Changes in extracellular space diffusion parameters in the cortex of the young adult and aged (28-month-old) rat after cardiac arrest. Diffusion curves were recorded in layer V and are superimposed on the increasing TMA^+ baseline due to ECS volume shrinkage. Diffusion parameters: volume fraction (α), tortuosity (λ), and nonspecific uptake k' are shown with representative curves prior to and after cardiac arrest.

extracellular matrix (ECM), the manner in which cells interact with the ECM, growth and trophic factor binding, the regulation of cell migration, axonal outgrowth, axonal branching, synaptogenesis, and metastasis. This means not only a lower overall "diffusivity" of the tissue because of the smaller extracellular pores, but also a loss of directionality of the diffusion because of the loss of anisotropy. In this way astrocytes can contribute to a learning mechanism in the hippocampus.

Tortuosity is influenced by many factors that we presently cannot separate. These might be: membrane barriers including neuronal and glial cell processes, myelin sheaths, macromolecules including the extracellular matrix, molecules with fixed negative surface charges, extracellular space size, and pore geometry. The present study, together with our recent studies, supports a role for the macromolecular content of the extracellular fluid (Prokopová *et al*., 1996) and for geometrical constraints, as an increase in tortuosity accompanies astrogliosis evoked by radiation injury (Syková *et al*., 1996), astrogliosis in grafted tissue (Roitbak *et al*., 1996), and myelination (Vořišek and Syková, 1997a).

Anisotropy in CC (Vořišek and Syková, 1997a; Mazel *et al*., 1998) and in hippocampus (Mazel *et al*., 1998) has been reported in young adult rats. Structural anisotropy in some regions of the brain has also been inferred from diffusion-weighted MRI (DW-MRI) measurements (Moseley *et al*., 1990). DW-MRI, which measures the ADC of water, cannot, however,

distinguish between the intra- and extracellular compartments, and therefore, these studies could not confirm the extent of anisotropy in the extracellular space. In the hippocampus, diffusion in the *y*- and *z* directions is significantly slower than in the *x* direction, as shown by the higher tortuosity in both the *y*- and *z*-axes (Table 1). We suppose that there are two main factors contributing to this anisotropy. First, most fiber systems in the hippocampus (Schaffer collaterals in CA1 and mossy fibers in CA3) run transversally. This would, similarly to the corpus callosum (Voříšek and Syková, 1997a), cause λ_y and λ_z to be significantly higher than λ_x. A second factor that might explain the difference is the typical arrangement of cellular aggregates in the hippocampus, including astrocytic processes and perineuronal nets, which might form diffusion barriers. This fine structure and the diffusion barriers appeared to be lost in our senescent rats. We have found significant changes in average tortuosity (averaging λ_x, λ_y, and λ_z) in the hippocampus of young and aged rats. This means that if a molecule spent a certain time moving in the *x* direction, then the same time in the *y* and *z* directions, it would travel a greater distance in aging brain.

Ischemia

The relative resistance of the immature brain to anoxia/ischemia is well known. On the other hand, here we have demonstrated that the time course of ionic and diffusion parameter changes in the ECS associated with cellular (particularly astrocytic) swelling is faster during maturation and aging. It has also been noted that there is an increase in the vulnerability of astrocytes to oxidative injury with age (Papadopoulos *et al*., 1997). Evidence for increased vulnerability includes an earlier onset of anoxic depolarization (signaling the massive redistribution of ions across brain cell membranes) (Voříšek and Syková, 1997b), and a diminished recovery of synaptic activity after anoxia in aging rats (Roberts *et al*., 1990; Roberts and Chih, 1995). There is also an age-related impairment of pH regulation that may affect the onset of anoxic depolarization and the recovery of brain function after anoxia (Roberts and Chih, 1997).

The observed substantial changes in diffusion parameters during and after progressive ischemia and anoxia in vivo could, therefore, affect diffusion in the ECS and aggravate the accumulation of ions, neurotransmitters, and metabolic substances during ischemia, thus contributing to irreversible ischemic brain damage. On the other hand, changes in the diffusion parameters may persist long after the ischemic event and affect extrasynaptic transmission in the CNS. Changes in the diffusion parameters may also, of course, affect the access to cellular elements of drugs used to treat nervous diseases.

Functional significance

If diffusion in the ECS is the underlying mechanism of extrasynaptic or “volume” transmission and intercellular, particularly neuron–glia, communication (Syková, 1997; Nicholson and Syková, 1998), then changes in ECS pore size would affect the movement of substances through this important communication channel. Anisotropy, which, particularly in the hippocampus and corpus callosum, may help to facilitate the diffusion of neurotransmitters and neuromodulators to regions occupied by their high affinity receptors, located extrasynaptically, might have crucial importance for the specificity of signal transmission. The importance of anisotropy for the “spill-over of glutamate,”, “cross-talk” between synapses, and for LTP and LTD has been proposed (Kullmann *et al*., 1996; Asztely *et al*., 1997). The observed decrease in ECS size and the loss of anisotropy in senescent rats could, therefore, lead to impaired cortical and, particularly, hippocampal function. They could also be responsible for the greater susceptibility of

aged brain to pathological events (particularly ischemia), the poorer outcome of clinical therapy, and the more limited recovery of affected tissue after insult.

Acknowledgments—This work was supported by grants GACR 309/96/0884, GACR 307/96/K226, IGA MZ 3423-3, GACR 309/97/K048. The aged rats were a gift from Troponwerke Research, Institute for Neurobiology, Köln, Germany.

REFERENCES

ADAMS, I. and JONES, D.G. Synaptic remodelling and astrocytic hypertrophy in rat cerebral cortex from early to late adulthood. *Neurobiol. Aging* **3:** 179–186, 1985.

AGNATI, L.F., ZOLI, M., STROMBERG, I., and FUXE, K. Intercellular communication in the brain: Wiring versus volume transmission. *Neuroscience* **69,** 711–726, 1995.

ASZTELY, F., ERDEMLI, G., and KULLMANN, D.M. Extrasynaptic glutamate spillover in the hippocampus: Dependence on temperature and the role of active glutamate uptake. *Neuron.* **18,** 281–293, 1997.

FUXE, K. and AGNATI, L.K. *Volume Transmission in the Brain: Novel Mechanisms for Neural Transmission*, Raven Press, New York, 1991.

GEINISMAN, Y., BONDAREFF, W., and DODGE, J.T., Hypertrophy of astroglial processes in the dentate gyrus of the senescent rat. *Am. J. Anat.* **153,** 537–543, 1978.

GOSS, J.R., FINCH, C.E., and MORGAN, D.G. Age-related changes in glial fibrillary acidic protein mRNA in the mouse brain. *Neurobiol. Aging* **12,** 165–170, 1991.

HARDINGTON, T.E. and FOSANG, A.J. Proteoglycans: Many forms and many functions. *FASEB J.* **6,** 861–870, 1992.

KULLMANN, D.M. and ASZTELY, F. Extrasynaptic glutamate spillover in the hippocampus; Evidence and implications. *Trends Neurosci.* **21,** 8–14, 1998.

KULLMANN, D.M., ERDEMLI, G., and ASZTELY, F. LTP of AMPA and NMDA receptor-mediated signals: Evidence for presynaptic expression adn extrasynaptic glutamate spill-over. *Neuron* **17,** 461–474, 1996.

LEHMENKÜHLER, A., SYKOVÁ, E., SVOBODA, J., ZILLES, K., and NICHOLSON, C. Extracellular space parameters in the rat neocortex and subcortical white matter during postnatal development determined by diffusion analysis. *Neuroscience* **55,** 339–351, 1993.

LINDSEY, J.D., LANDFIELD, P.W., and LYNCH, G. Early onset and topographical distribution of hypertrophied astrocytes in hippocampus of aging rats: A quantitative study. *J. Gerontol.* **34,** 661–671, 1979.

MARGOLIS, R.K. and MARGOLIS, R.U. Nervous tissue proteoglycans. *Experientia* **49,** 429–466, 1993.

MAZEL, T., ŠIMONOVÁ, Z., and SYKOVÁ, E. Diffusion heterogeneity and anisotropy in rat hippocampus. *Neuroreport*, **9,** 1299–1304, 1998.

McBAIN, C.J., TRAYNELIS, S.F., and DINGLEDINE, R. Regional variation of extracellular space in the hippocampus. *Science* **249,** 674–677, 1990.

MOSELEY, M.E., COHEN, Y., KUCHARCZYK, J., MINTOROVITCH, J., ASAGARAI, H.S., WENDLAND, M.F., TSURUDA, J., and NORMAN, D. Diffusion-weighted MR imagining of anisotropic water diffusion in cat central nervous system. *Radiology* **176,** 439–445, 1990.

NICHOLS, N.R., DAY, J.R., LAPING, N.J., JOHNSON, S.A., and FINCH, C.E. GFAP mRNA increases with age in rat and human brain. *Neurobiol. Aging* **14,** 421–429, 1993.

NICHOLSON, C. Dynamics of the brain cell microenvironment. *Neurosci. Res. Program Bull.* **18,** 177–322, 1980.

NICHOLSON, C. and PHILLIPS, J.M. Ion diffusion modified by tortuosity and volume fraction in the extracellular microenvironment of the rat cerebellum. *J. Physiol. (Lond).* **321,** 225–257, 1981.

NICHOLSON, C. and SYKOVÁ, E. Extracellular space structure revealed by diffusion analysis. *Trends Neurosci.* **21,** 207–215, 1998.

NORENBERG, M.D. Astrocyte responses to CNS injury. *J. Neuropathol. Exp. Neurol.* **53,** 213–220, 1994.

O'CALLAGHAN, J.P. and MILLER, D.B. The concentration of glial fibrillary acidic protein increases with age in the mouse and rat brain. *Neurobiol. Aging* **12,** 171–174, 1991.

PAPADOPOULOS, M.C., KOUMENIS, I.L., YUAN, T.Y., and GIFFARD, R.G. Increasing vulnerability of astrocytes to oxidative injury with age despite constant antioxidant defenses. *Neuroscience* **82,** 915–925, 1997.

PROKOPOVÁ, Š., NICHOLSON, C., and SYKOVÁ, E. The effect of 40-dDa or 70-kDa dextran and hyaluronic acid solution on extracellular space tortuosity in isolated rat spinal cord. *Physiol. Res.* **45,** P28, 1996.

PROKOPOVÁ, Š., VARGOVÁ, L., and SYKOVÁ, E. Heterogeneous and anisotropic diffusion in the developing rat spinal cord. *Neuroreport.* **8,** 3527–3532, 1997.

RAPP, P.R. and GALLAGHER, M. Preserved neuron number in the hippocampus of aged rats with spatial learning deficits. *Proc. Natl. Acad. Sci. USA* **93,** 9926–9930, 1996.

RICE, M.E., OKADA, Y.C. and NICHOLSON, C. Anisotropic and heterogeneous diffusion in the turtle cerebellum: Implications for volume transmission. *J. Neurophysiol.* **70,** 2035–2044, 1993.

ROBERTS, E.L. and CHIH, C.P. Age-related alterations in energy metabolism contribute to the increased vulnerability of the aging brain to anoxic damage. *Brain Res.* **678,** 83–90, 1995.

ROBERTS, E.L. and CHIH, C.P. The influence of age on pH regulation in hippocampal slices before, during, and after anoxia. *J. Cereb. Blood Flow Metab.* **17,** 560–566, 1997.

ROBERTS, E.L., ROSENTHAL, M., and SLICK, T.J. Age-related modifications of potassium homeostasis and synaptic transmission during and after anoxia in rat hippocampal slices. *Brain Res.* **514,** 111–118, 1990.

ROITBAK, T., MAZEL, T., ŠIMONOVÁ, Z., HARVEY, A., and SYKOVÁ, E. Extracellular space volume and geometry in rat fetal brain grafts. *Eur. J. Neurosci. (Suppl.),* **9,** 37, 1996.

SYKOVÁ, E. Extracellular K^+ accumulation in the central nervous system. *Prog. Biophys. Mol. Biol.* **42,** 135–189, 1983.

SYKOVÁ, E. *Ionic and Volume Changes in the microenvironment of Nerve and Receptor Cells*, Springer Verlag, Heidelberg, 1992.

SYKOVÁ, E. The extracellular space in the CNS: Its regulation, volume and geometry in normal and pathological neuronal function. *Neuroscientist* **3,** 28–41, 1997.

SYKOVÁ, E., SVOBODA, J., POLÁK, J., and CHVÁTAL, A. Extracellular volume fraction and diffusion characteristics during progressive ischemia and terminal anoxia in the spinal cord of the rat. *J. Cereb. Blood Flow Metab.* **14,** 301–311, 1994.

SYKOVÁ, E., SVOBODA, J., ŠIMONOVÁ, Z., LEHMEHKÜHLER, A., and LASSMANN, H. X-irradiation-induced changes in the diffusion parameters of the developing rat brain. *Neuroscience* **70,** 597–612, 1996.

VOŘÍŠEK, I. and SYKOVÁ, E. Evolution of anisotropic diffusion in the developing rat corpus callosum. *J. Neurophysiol.* **78,** 912–919, 1997a.

VOŘÍŠEK, I. and SYKOVÁ, E. Ischemia-induced changes in the extracellular space diffusion parameters, K^+ and pH in the developing rat cortex and corpus callosum. *J. Cereb. Blood Flow Metab.* **17,** 191–203, 1997b.

WICKELGREN, I. Is hippocampal cell death a myth? *Science* **271,** 1229, 1996.